AD-A069 081 ARMY ARMAMENT RESEARCH AND DEVELOPMENT COMMAND ABERD--ETC F/G 7/4
TRAJECTORY CALCULATIONS FOR THE REACTION OF O ATOMS WITH OH.(U)
MAR 79 A GAUSS

UNCLASSIFIED ARBRL-TR-02149 SBIE-AD-E430 229 NL

1 OF 1
AD A069 081

END
DATE FILMED
7-79
DDC

UNCLASSIFIED

SECURITY CLASSIFICATION OF THIS PAGE (When Data Entered)

| REPORT DOCUMENTATION PAGE | READ INSTRUCTIONS BEFORE COMPLETING FORM |
|---|---|
| 1. REPORT NUMBER: TECHNICAL REPORT ARBRL-TR-02149 | 2. GOVT ACCESSION NO. / 3. RECIPIENT'S CATALOG NUMBER |
| 4. TITLE (and Subtitle): Trajectory Calculations for the Reaction of O Atoms With OH | 5. TYPE OF REPORT & PERIOD COVERED: BRL Report |
| | 6. PERFORMING ORG. REPORT NUMBER |
| 7. AUTHOR(s): Arthur Gauss, Jr. | 8. CONTRACT OR GRANT NUMBER(s) |
| 9. PERFORMING ORGANIZATION NAME AND ADDRESS: US Army Ballistic Research Laboratory, ATTN: DRDAR-BLB, Aberdeen Proving Ground, MD 21005 | 10. PROGRAM ELEMENT, PROJECT, TASK AREA & WORK UNIT NUMBERS: RDT&E 1L161102AH43 |
| 11. CONTROLLING OFFICE NAME AND ADDRESS: US Army Armament Research & Development Command, US Army Ballistic Research Laboratory, ATTN: DRDAR-BL, APG, MD 21005 | 12. REPORT DATE: MARCH 1979 |
| | 13. NUMBER OF PAGES: 25 |
| 14. MONITORING AGENCY NAME & ADDRESS (if different from Controlling Office) | 15. SECURITY CLASS. (of this report): Unclassified |
| | 15a. DECLASSIFICATION/DOWNGRADING SCHEDULE |

16. DISTRIBUTION STATEMENT (of this Report)

Approved for public release; distribution unlimited

17. DISTRIBUTION STATEMENT (of the abstract entered in Block 20, if different from Report)

O + OH yields H + O2.

18. SUPPLEMENTARY NOTES

O + O'H yields O' + OH,

O + OH

19. KEY WORDS (Continue on reverse side if necessary and identify by block number)

Chemical reactions, $OH+O \rightarrow H+O_2$ reaction, chemical trajectory calculations, Monte Carlo trajectory calculations, LEPS potential energy surface, vibrational-rotational excitation in exothermic reactions, Sato parameters, Morse potentials

20. ABSTRACT (Continue on reverse side if necessary and identify by block number) (hmm)

Trajectory calculations have been used to calculate cross sections and specific rate constants for the two channels of the O+OH, reaction. Channel 1 is the exchange reaction O+O' H+O' +OH, channel 2 the reaction $O+OH \rightarrow H+O_2$. From the specific rates, estimates of the overall thermal rate constants are calculated. The minimum thermal rate constant calculated for the channel 2 reaction is $(5.4 \pm 0.7) \times 10^{-11}$ $\frac{cm^3}{molecule\ sec.}$ at 300°K, a value within error limits of (over)

(5.4 + or - 0.7) x 10 to the -11th power cc/molecule sec. at 300°K,

DD FORM 1 JAN 73 1473 EDITION OF 1 NOV 65 IS OBSOLETE

UNCLASSIFIED

SECURITY CLASSIFICATION OF THIS PAGE (When Data Entered)

that recommended by Wilson. The temperature dependence of this thermal rate constant, although higher, follows the shape of the curve of Kurzius and Boudart. The exchange reaction (channel 1) is estimated to be one third to one fifth as probable as the channel 2 reaction.

## TABLE OF CONTENTS

# I. INTRODUCTION

In the reaction of O atoms with OH two reactions are possible. One is the reaction $O+OH \rightarrow H+O_2$ (channel 2); the other is the exchange reaction $O+O' H \rightarrow OH+O'$ (channel 1). This report will concentrate on the channel 2 reaction but some data on channel 1 will also be presented.

There have been a number of experimental measurements[1-4] of the thermal rate constant for the $O+OH \rightarrow H+O_2$ reaction, all at relatively low temperatures (near 300°K). The minimum thermal rate constant (neglecting reaction complexes, see Section III) calculated here from trajectories agrees near 300°K with several experimental results[1-3] and the recommended value[5]. However, this calculated rate constant is certainly low because of the long-lived complex trajectories which the integrator of the classical trajectory program (CLASTR[6]) cannot follow (see Section III). If the decision of the integrator is taken as correct for these complex trajectories, then the rate constant calculated will be two to three times the minimum rate. If all the complex trajectories are assumed to react to form $H+O_2$ (the worst possible case), then the rate calculated for channel 2 will be a little more than three times the minimum rate.

Kurzius and Boudart[7] have formulated an empirical model to predict the rate constant for the $O+OH \rightarrow H+O_2$ reaction over a wide temperature range (see Fig. 7). Also the reverse rate constant and equilibrium constant data have been used to predict the rate constant over a wide range of temperature[8]. The minimum rate constant calculated here is generally higher than these two determinations[7,8] (by a factor of four). The calculated minimum rate shows the same flat temperature dependence (Figure 7).


1. M.A.A. Clyne and B.A. Thrush, Proc. Roy. Soc. (London) A275, 544 (1963).
2. F. Kaufman, Ann. Geophys. 20, 106 (1964).
3. J.E. Breen and G.P. Glass, J. Chem. Phys., 52, 1082 (1970).
4. A.A. Westenberg, N. de Haas, and J.M. Roscoe, J. Phys. Chem., 74, 3431 (1970).
5. W.E. Wilson Jr., J. Phys. Chem. Ref. Data 1, 535 (1972).
6. CLASTR is program No. 229 in the Quantum Chemistry Program Exchange Catalog (QCPE, Indiana University Chemistry Department).
7. S.C. Kurzius and M. Boudart, Combust. & Flame, 12, 477 (1968).
8. D.L. Baulich, D.D. Drysdale, and D.G. Horne, Fourteenth Symposium on Combustion (Combustion Institute, Pittsburg, 1973), p. 107.

All the calculations have been performed on a modified LEPS surface (Surface I'') similar to the surface (Surface I) used in the treatment of the $H+O_2 \rightarrow OH+O$ reaction[9]. Modification involves only a slight change in the Sato parameter and addition of a constant to the potential as a whole. The potential contours of Surfaces I and I'' are very similar over all values of the H-O-O angle $\theta$.

The minimum thermal rate constant for the exchange reaction (channel 1) is considerably less than for the $H+O_2$ channel. It varies from one fifth to one third the channel 2 rate.

## II. POTENTIAL SURFACE

The potential surface used in these calculations is a modified LEPS surface similar to one employed for the $H+O_2 \rightarrow OH+O$ reaction. The general form of the LEPS surface[10] is

$$V = Q_1' + Q_2' + Q_3' - (\alpha_1'^2 + \alpha_2'^2 + \alpha_3'^2 - \alpha_1'\alpha_2' - \alpha_1'\alpha_3' - \alpha_2'\alpha_3')^{1/2} + D_2^e$$

where

$$Q_i' = \frac{Q_i}{1+\Delta_i} = \frac{D_i^e}{4(1+\Delta_i)} \left\{ \left(3+\Delta_i\right) e^{-2\beta_i(r_i-r_{io})} - \left(2+6\Delta_i\right) e^{-\beta_i(r_i-r_{io})} \right\}$$

and

$$\alpha_i' = \frac{\alpha_i}{1+\Delta_i} = \frac{D_i^e}{4(1+\Delta_i)} \left\{ \left(1+3\Delta_i\right) e^{-2\beta_i(r_i-r_{io})} - \left(6+2\Delta_i\right) e^{-\beta_i(r_i-r_{io})} \right\}$$

$i = 1,2,3$ .

The coordinate system defining $r_1$, $r_2$ and $r_3$ together with certain other variables is pictured in Fig. 1. The zero of energy for this surface (Surface I'') occurs for infinite separation in the channel O+OH. The Sato parameter is given by

$$\Delta = \left(1-e^{-\left(x_a/b\right)^2}\right) \times \left\{ 0.53(\sin 2Th)^2 - 0.25(\text{Cos } Th)^2 + 0.2(\pi/2)^2 \right\}$$

9. A. Gauss, Jr., J. Chem. Phys. 68, 1689 (1978).
10. J.T. Muckerman, J. Chem. Phys. 56, 2997 (1972).

where

$$b = 0.6 \times 10^{-8} \text{ cm.}$$

$$Th = \text{Arcsin}\left(\frac{r_2}{x_a} \sin\theta\right)$$

and

$$x_a = \left(r_2^2 + r_3^2/4 - r_2\, r_3 \cos\theta\right)^{\frac{1}{2}} .$$

The equilibrium position for this surface is very close to that of Surface I at $r_2 = 0.97$Å, $r_3 = 1.21$Å, $\theta = 107°$ (H-O-O angle). The experimental values[11] are $r_2 = 0.985$Å, $r_3 = 1.36$Å, and $\theta = 106°$. The variation of this potential surface with the H-O-O angle is shown in Figure 2. Also plotted here for comparison are the ab initio results of Gole and Hayes[12].

Potential energy contour plots are presented in Figures 3,4, and 5 for $\theta = 180°$, 108° and 80° respectively. Note that these contours have the potential zero in the separated $H+O_2$ channel (for $r_3=r_{30}$ as $r_1$ and $r_2 \to \infty$). The zero of the potential Surface I'' is in the separated O+OH channel and thus differs from the surface (called Surface I')[13] pictured in Figures 3, 4 and 5 by a constant $(D_2^e - D_3^e)$.

Surface I had an infinity in the derivative in the linear configuration. The change in the angular (Th) dependence for Surfaces I' and I'' remedies this difficulty.

The Surface I' (pictured in Figures 3, 4 and 5) has been used for dynamics calculations of the $H+O_2$ reaction[13]. Trajectory results on Surface I' closely match those on Surface I. The system is rarely in the linear or near linear configuration even on Surface I' and thus problems in this configuration on Surface I appear unimportant to the trajectory results.

---

11. J.F. Ogilvie, Can. J. Spect., 19, 171 (1973).
12. J.L. Gole and E.F. Hayes, J. Chem. Phys. 57, 360 (1972).
13. A. Gauss, Jr., "The $H+O_2 \to OH+O$ Reaction, A Comparison of Potential Surfaces", ARBRL-TR-, February 1979 (to be published).

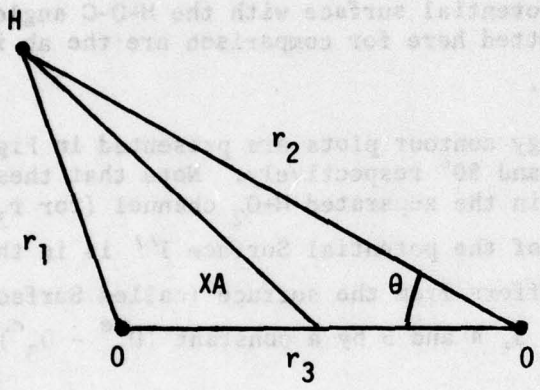


**Figure 1.** The internuclear coordinates $r_1$, $r_2$ and $r_3$ and the H-O-O angle ($\theta$) are defined as shown. The angle "Th" and the distance "$x_a$" are displayed on the diagram.

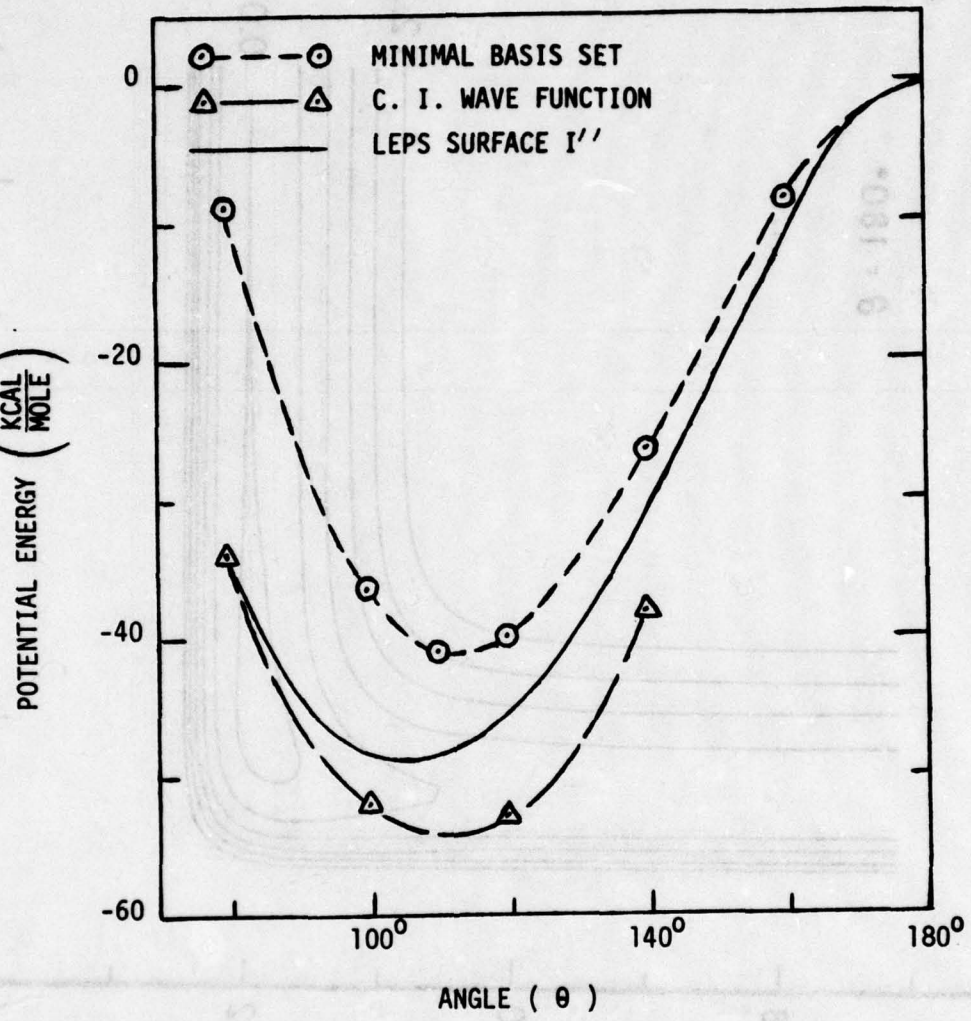


Figure 2. Comparison (at $r_2$ = 0.96Å, $r_3$ = 1.23Å) of the angular dependence of the LEPS potential energy Surface I'' with the ab initio surfaces calculated by Gole and Hayes.

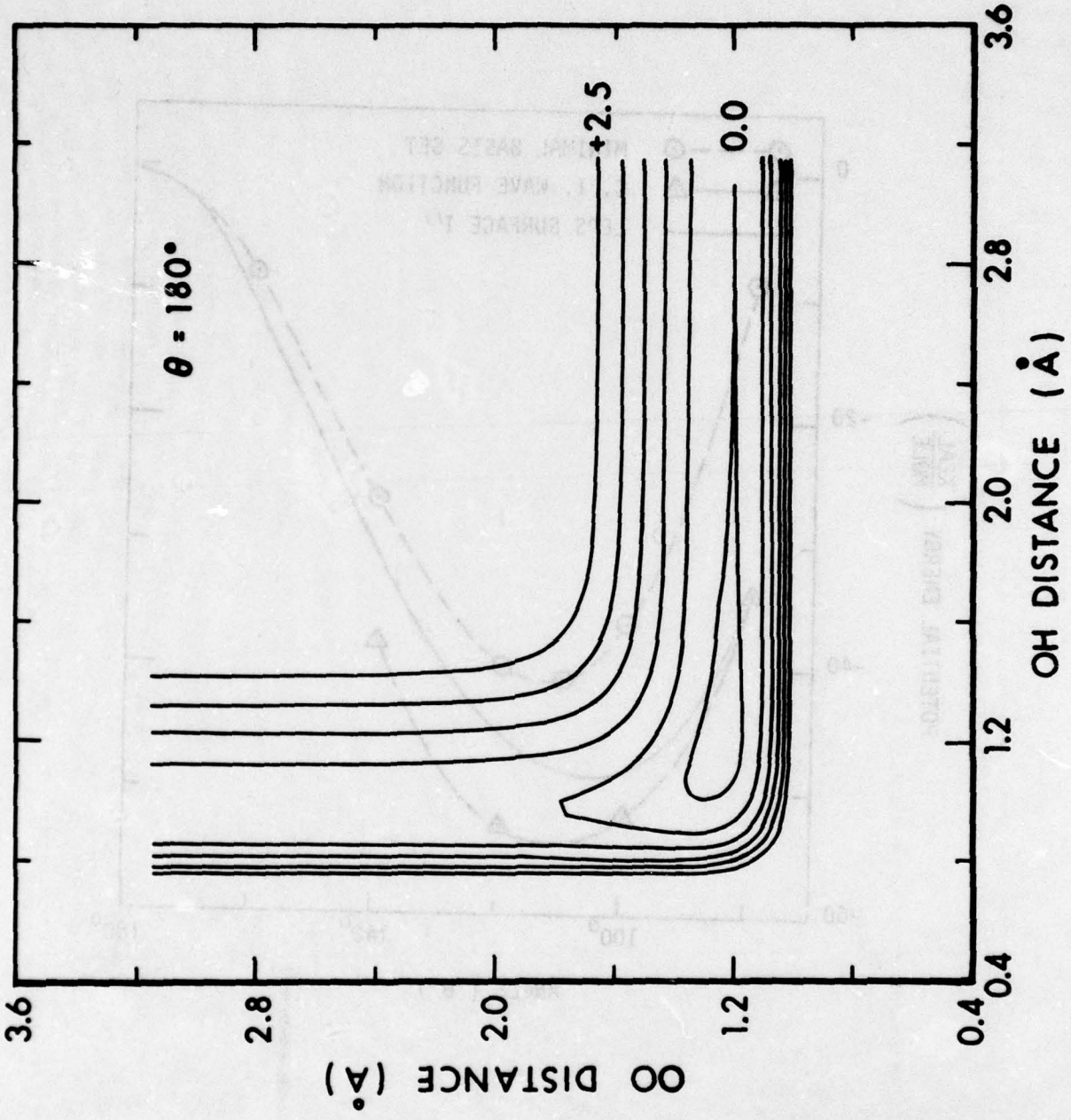


Figure 3. Contour diagram of the LEPS potential Surface I′ for θ=180°. Contours labelled in eV. with 0.5 eV. spacing. This surface differs only by an additive constant ($D_2^e$-$D_3^e$) from Surface I′′ used in this O + OH study.

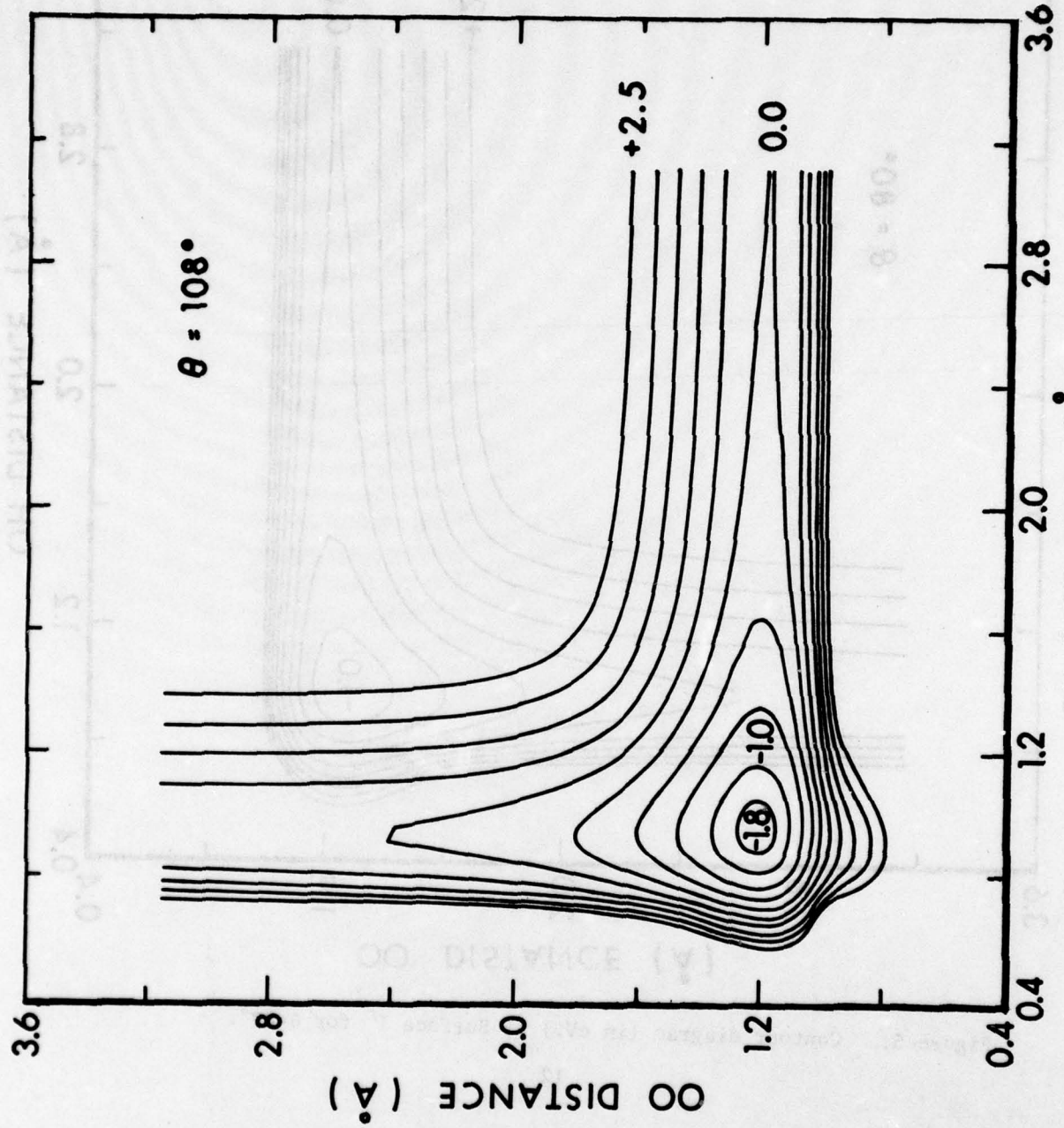


Figure 4. Contour diagram (in eV.) of Surface I′ for θ=108°.

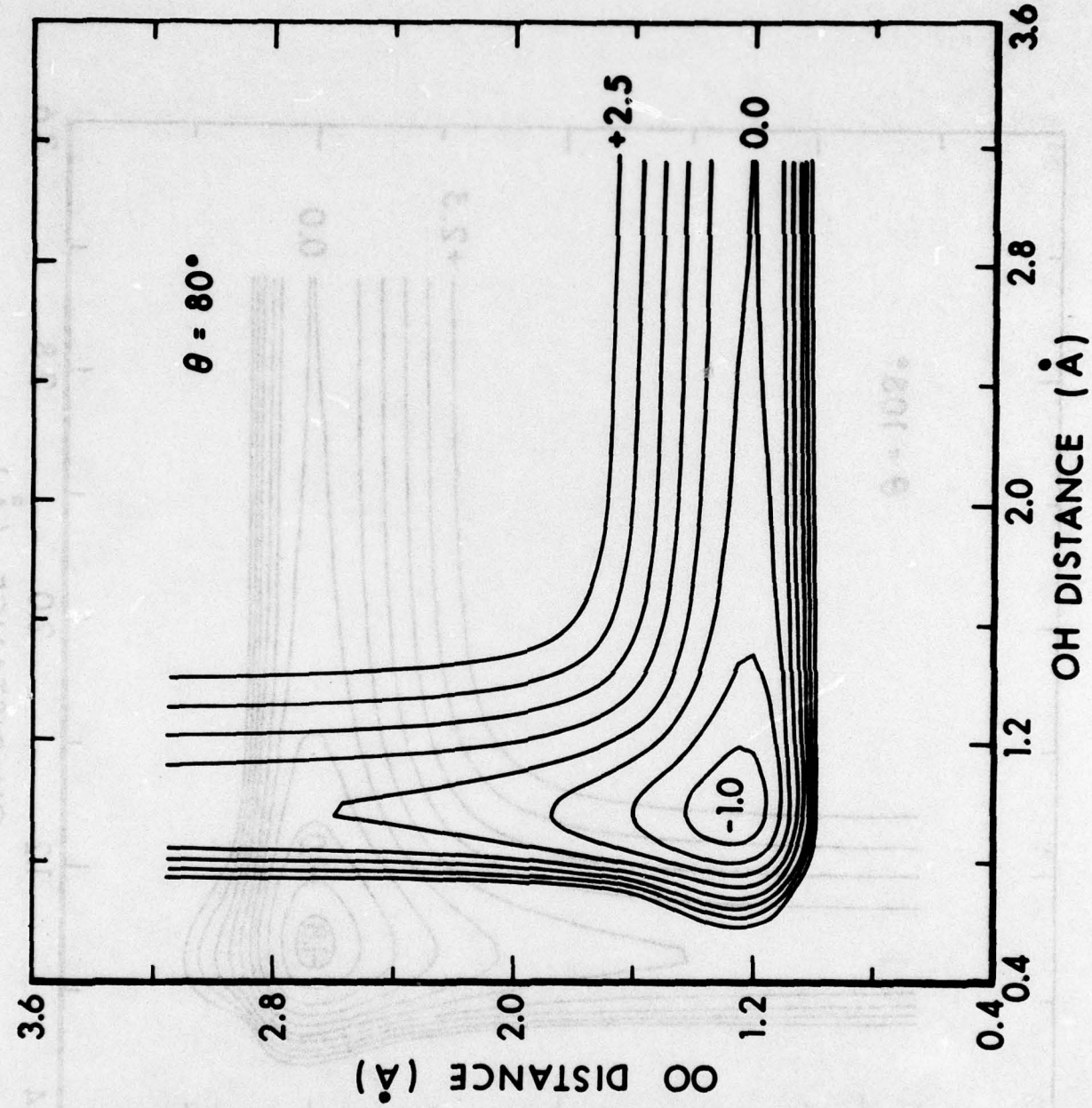


Figure 5. Contour diagram (in eV.) of Surface I′ for θ=80°.

## III. TRAJECTORY CALCULATIONS FOR O+OH

Trajectory results are summarized in Table I. All trajectories were run for OH in the ground state (v=0, J=0). Table I displays the results as a function of relative translational energy ($E_R$). Three main types of trajectory events are recognized: reactive, non-reactive, and complex. The reactive events can be subdivided into reactive channel 1 (R1) and reactive channel 2 (R2) events. R1 is the exchange reaction, reaction R2 gives the $H+O_2$ products. Both reactive and nonreactive trajectories are back integrable, using the back integration option of the CLASTR code. Both energy and angular momentum are conserved. Complex trajectories are not back integrable, although energy and angular momentum are conserved. In Table II the complex trajectories have been further subdivided into reactive complexes and non-reactive complexes according to the decision of the CLASTR integrator.

TABLE I. A summary of the reactive and complex trajectories is presented. The reactions are subdivided into channel 1 (R1) and channel 2 (R2) reactive events. The total number of trajectories is given for each translational energy ($E_R$). The OH is initially in the v=0, J=0 state.

| $E_R$ $\left(\frac{\text{kcal}}{\text{mole}}\right)$ | Reactions | | Total Complexes | Total Trajs |
|---|---|---|---|---|
| | R1 | R2 | | |
| 2 | 14 | 55 | 117 | 500 |
| 5 | 16 | 69 | 94 | 500 |
| 10 | 13 | 35 | 24 | 500 |
| 15 | 16 | 27 | 15 | 500 |

The minimum cross sections for the channel $O+OH \rightarrow H+O_2$ are shown in Figure 6. Minimum cross sections are calculated from the R2 events only, complexes are assumed to be non-reactive. The minimum cross sections have here been plotted as a function of translational energy. A simple straight line fits the data well ($S_r = 0.3\ E_R + 6.5$). From this straight line fit the minimum specific rate constant ($k_{oo}$) has been evaluated at four temperatures 300°K, 400°K, 1600° and 2500°K (See Table III). Evaluation of the specific rate constant at the lower temperatures (300 and 400°K) assumes that the cross section has been correctly extrapolated into the region of low translational energy

TABLE II. The complex trajectories tabulated in Table I are here subdivided into reactive and non-reactive groups using the decision of the CLASTR integrator. The complex reactive events are further subdivided into channel 1 reactive events (CR1) and channel 2 reactive events (CR2).

| $E_R$ $\left(\frac{\text{kcal}}{\text{mole}}\right)$ | Total Complexes | Reactive Complexes CR1 | CR2 | Non-Reactive Complexes |
|---|---|---|---|---|
| 2 | 117 | 11 | 76 | 30 |
| 5 | 94 | 4 | 50 | 40 |
| 10 | 24 | 2 | 14 | 8 |
| 15 | 15 | 2 | 3 | 10 |

TABLE III. The minimum specific rate constant for channel 2 is shown for four temperatures (300, 400, 1600 and 2500°K). The units of the rate constant here are $cm^3$/molecule sec.

| Temperature (°K) | Minimum Specific Rate Constant ($cm^3$/molecule sec.) |
|---|---|
| 300 | $(5.4 \pm 0.7) \times 10^{-11}$ |
| 400 | $(6.1 \pm 0.8) \times 10^{-11}$ |
| 1600 | $(9.3 \pm 1.2) \times 10^{-11}$ |
| 2500 | $(9.2 \pm 1.3) \times 10^{-11}$ |

(< 2 kcal/mole). If rotational energy has little effect on the specific rate ($k_{oo}$), then it can reasonably be taken as equal to the total thermal rate constant (k) particularly for the lower temperatures (< 1000°K). Vibrational effects may have to be considered at very high temperatures, but the upper (v > 0) vibrational levels of OH are not highly populated since they are widely separated (> 10 kcal/mole). Neglecting rotational

and vibrational effects the minimum specific rate constant $k_{oo}$ is taken to be equivalent to the minimum overall thermal rate constant (k) and is plotted versus temperature in Figure 7. Observe that the temperature dependence is virtually the same as the empirical estimates of other workers[7,8]; however, the minimum theoretical rate is somewhat high.

Another theoretical rate for the $O+OH \rightarrow H+O_2$ reaction can be calculated assuming that the decision of the CLASTR integrator is correct for the complex trajectories (Table III). The total number of reactions are then taken as (R2 + CR2). The cross section curve for this case shown in Fig. 6 is a simple exponential fit $\left( S_r = A e^{-BE_R}, A = 17\text{Å}^2, B = 1.22 \text{ (kcal/mole)}^{-1} \right)$ to the trajectory data. The total thermal rate for this case is shown in Figure 7. The maximum possible rate (assuming all complexes are channel 2 events) would be about one-third more than the rate assuming (R2 + CR2) as the correct number of reactions.

The CLASTR program provides us with some interesting information on the vibrational and rotational excitation of the $O_2$ product molecule. At $2 \frac{\text{kcal}}{\text{mole}}$ relative translational energy most of the energy goes into $O_2$ vibrational energy (~ 43%) with the rest equally divided between rotation and translation (~ 28 to 29% each). At 15 kcal/mole relative translational energy most of the energy goes into $O_2$ rotation (~ 47%) with about equal amounts in vibration and translation (~ 26 to 27% each). The absolute energy in vibration stays nearly constant (~ 8-9 kcal/mole) over all translational energies. This vibrational energy corresponds to $O_2$ excited to the first or second vibrational level.

The exchange reaction is much less probable than the channel 2 reaction. From the data of Tables I and II cross sections may be derived. The minimum cross sections for this reaction are nearly constant over all translational energies; the average is $S_{r_{oo}} = (1.29 \pm .33)\text{Å}^2$. The cross section points and average are shown in Figure 8. This cross section yields the minimum specific rate constants shown in Table IV. Neglecting rotational and vibrational effects these specific rates may be taken as the overall thermal rates. Over the temperature range 300°K - 2500°K the exchange rate varies from one-fifth to one-third the rate in channel 2 (see Figure 9).

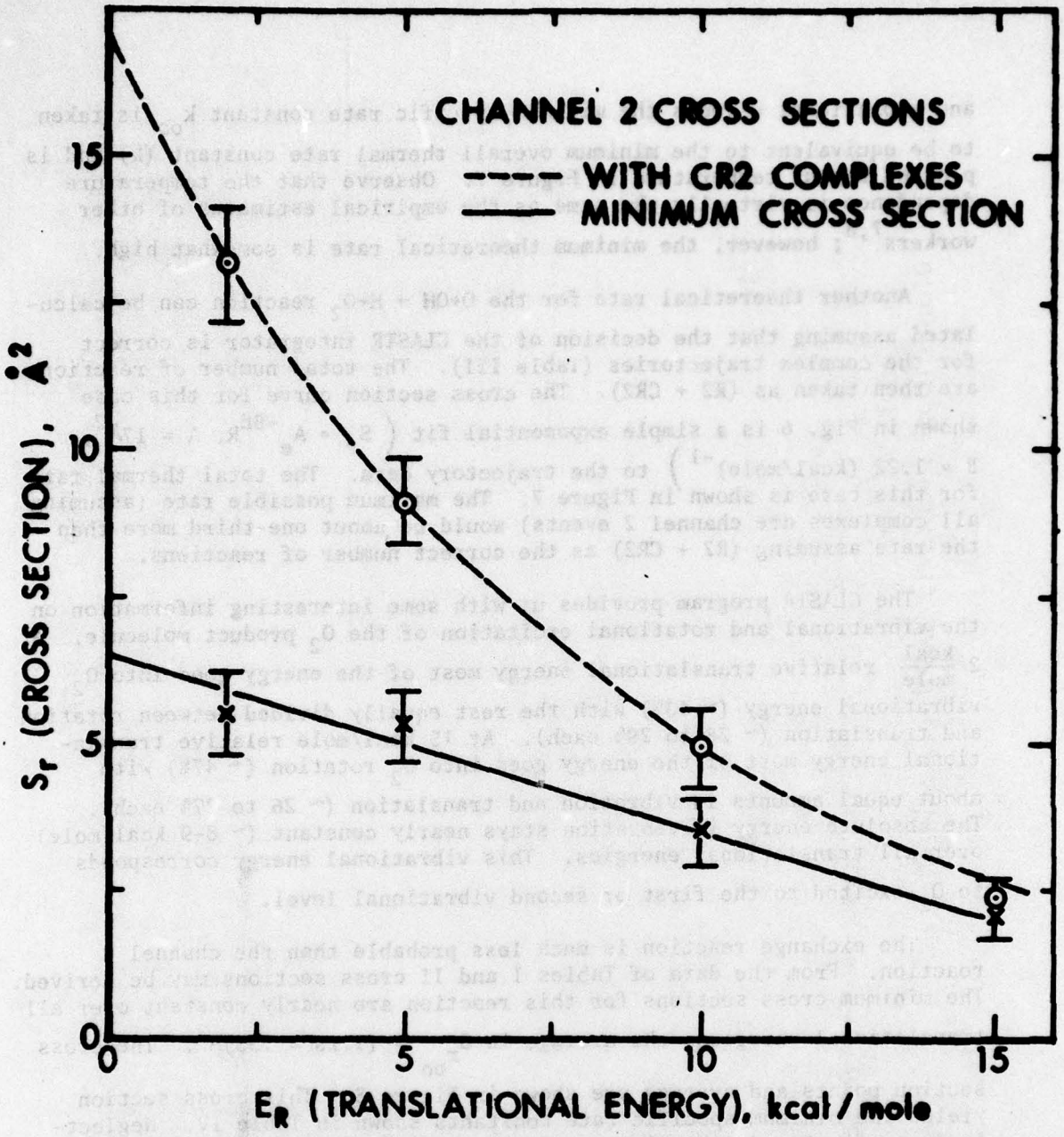


Figure 6. The cross sections ($S_r$) for channel 2 as a function of translational energy ($E_R$) are shown. The minimum cross section is fit with a straight line $S_r = -0.3\,E_R + 6.5$. The dashed line is a simple exponential fit $\left(S_r = Ae^{-BE_R},\ A=17\text{Å}^2,\ B=0.122\left(\frac{\text{kcal}}{\text{mole}}\right)^{-1}\right)$ to the data including both channel 2 reactions (R2) and channel 2 reactive complexes (CR2). Maximum impact parameters vary from 3.5 to 4.0Å.

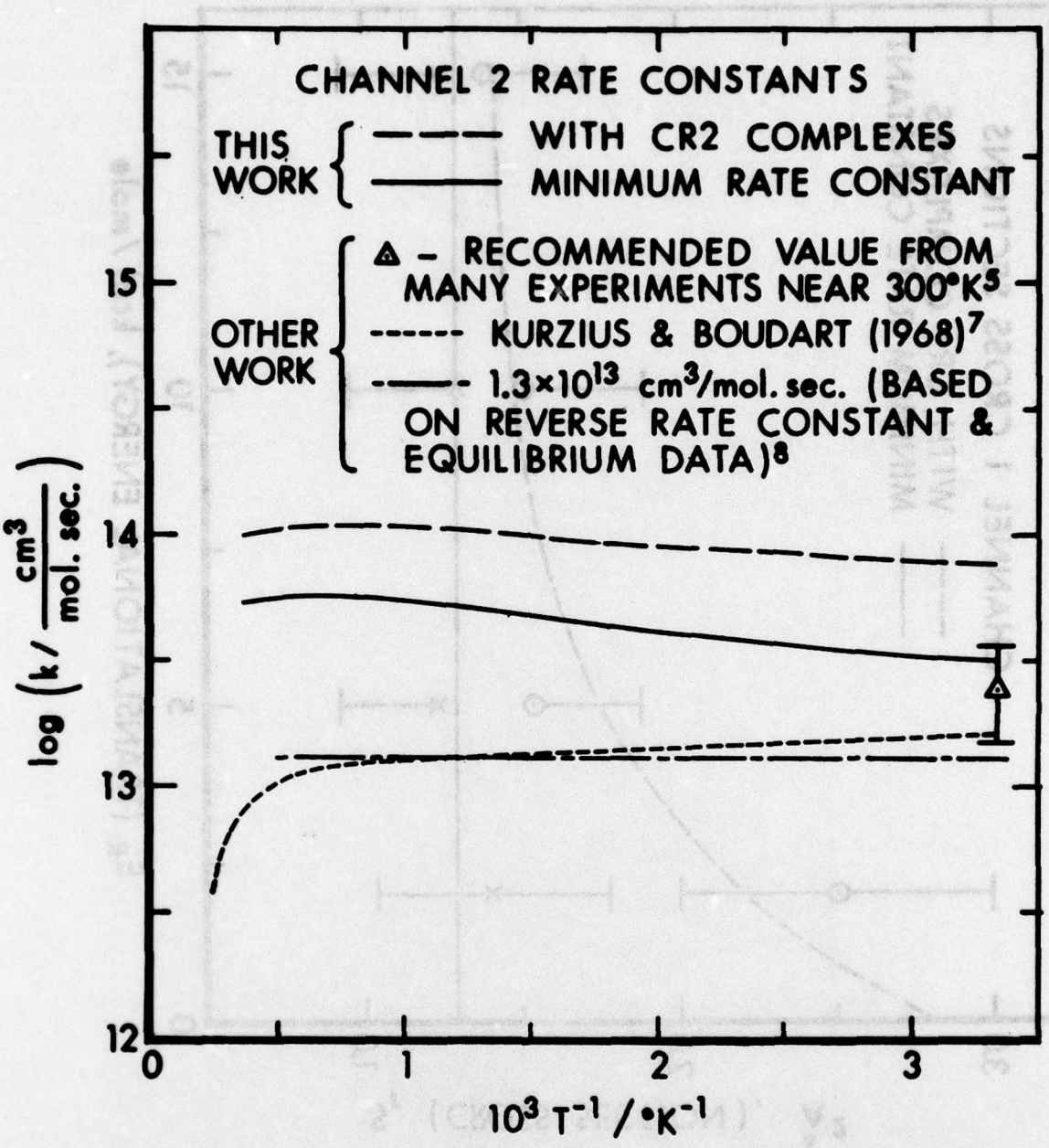


Figure 7 The rate constants (channel 2) as a function of temperature from trajectory calculation as well as from other sources[5,7,8] are shown. All the rate constant curves show little change with temperature over the range 300-2000°K. Note the units $cm^3$/mol. sec. on the rate constant.

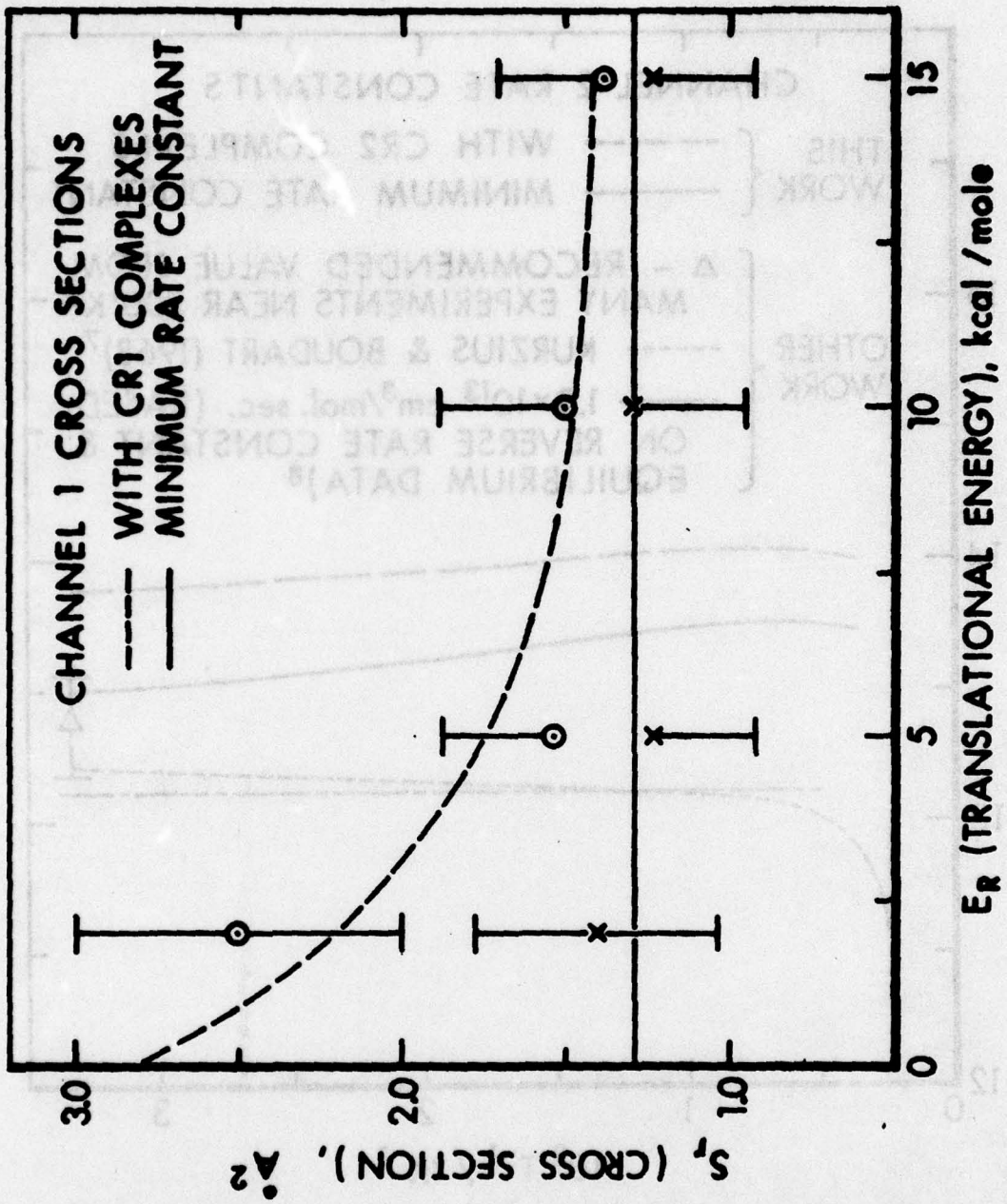


Figure 8. The cross sections ($S_r$) for channel 1 are shown as a function of translational energy ($E_R$). The minimum cross section is fit by the constant $S_r = (1.29 \pm .33)\text{Å}^2$. The dashed line is simple function ($S_r = A(1+e^{-BE_R})$, $A=1.4\text{Å}^2$, $B=2.77\ (\text{kcal/mole})^{-1}$) fitting the cross section data including both channel 1 reactions (R1) and channel 1 reactive complexes (CR1).

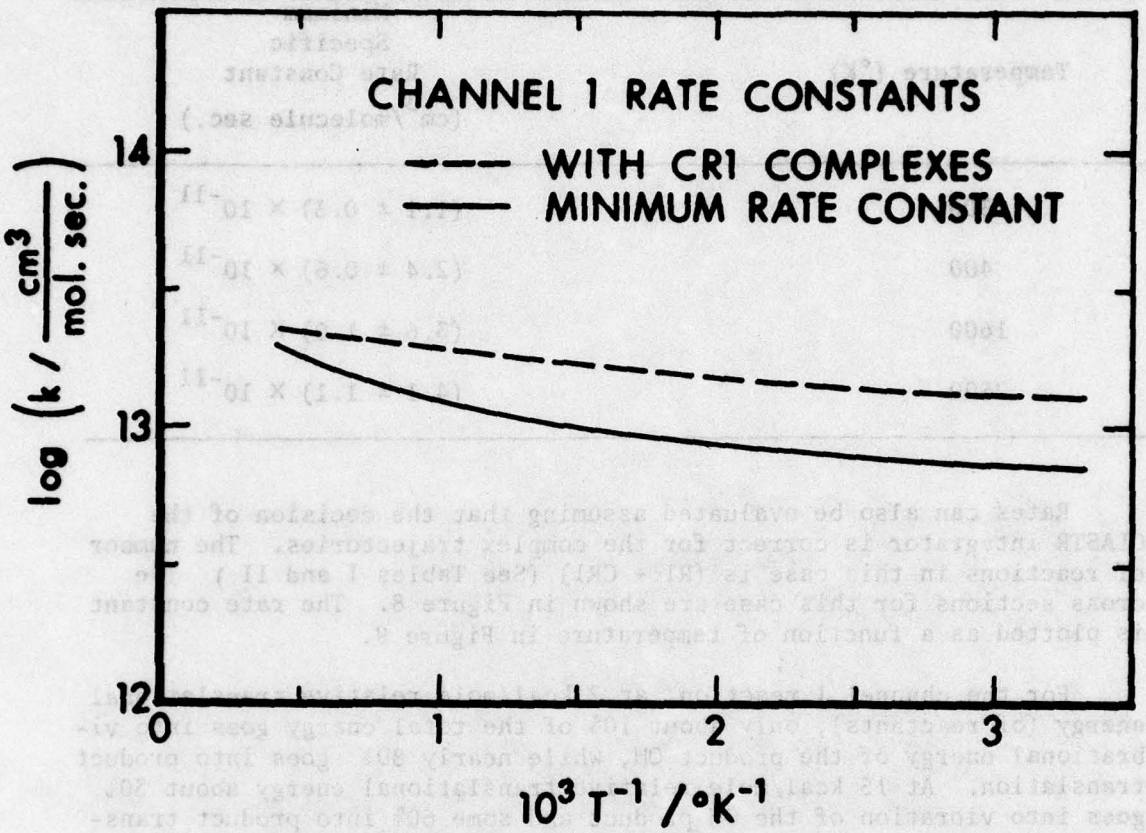


**Figure 9.** The rate constants (channel 1) as a function of temperature from trajectory calculations are pictured. Note the units $cm^3$/mol. sec. on the rate constant.

TABLE IV. The minimum specific rate constant for channel 1 is shown at four temperatures (300, 400, 1600 and 2500°K). The units of the rate constant here are $cm^3$/molecule sec.

| Temperature (°K) | Minimum Specific Rate Constant ($cm^3$/molecule sec.) |
|---|---|
| 300 | $(1.1 \pm 0.3) \times 10^{-11}$ |
| 400 | $(2.4 \pm 0.6) \times 10^{-11}$ |
| 1600 | $(3.6 \pm 1.0) \times 10^{-11}$ |
| 2500 | $(4.1 \pm 1.1) \times 10^{-11}$ |

Rates can also be evaluated assuming that the decision of the CLASTR integrator is correct for the complex trajectories. The number of reactions in this case is (R1 + CR1). (See Tables I and II.) The cross sections for this case are shown in Figure 8. The rate constant is plotted as a function of temperature in Figure 9.

For the channel 1 reaction, at 2 kcal/mole relative translational energy (of reactants), only about 10% of the total energy goes into vibrational energy of the product OH, while nearly 80% goes into product translation. At 15 kcal/mole relative translational energy about 30% goes into vibration of the OH product and some 60% into product translation. Product rotational energy is always rather small, typically 10 to 15 percent. Absolute product translational energy is nearly constant at (18 ± 2) kcal/mole over all relative translational energies.

## IV. DISCUSSIONS AND CONCLUSIONS

Several assumptions have been made in deriving estimates of the thermal rate constants. Among these are the neglect of rotational and vibrational effects. These effects should be analyzed in the future. In particular the reaction OH(v=1)+O should be examined as there has been recent experimental work[14,15] on this reaction.

14. J.E. Spencer and G.P. Glass, Internat. J. of Chem. Kinetics, IX, 111 (1977).
15. J.E. Spencer, H. Endo, and G.P. Glass, Sixteenth Symposium on Combustion (Combustion Institute, Pittsburg, 1977) p. 829.

A new improved LEPS potential surface for $HO_2$ has recently been derived[13]. It uses two Sato parameters and fits the force constants of the $HO_2$ complex well. This surface has recently been used for dynamics calculations[13] on the $H+O_2 \rightarrow OH+O$ reaction. A few preliminary calculations using this surface for the O+OH reaction indicate that it yields cross sections similar to those for the Surface I'' used in this paper. However, many more calculations are in order.

The low temperature rate constants (at 300 and 400°K) are derived by extrapolating the cross section curve to low relative translational energies. Trajectory calculations should be run at these low translational energies to check the extrapolated curve.

Only five hundred trajectories were run for each translational energy because of the large amounts of computer time required. Fifty trajectories at 2 kcal/mole take some 700 to 800 sec. (with back integration) on the CDC 7600. Even at 15 kcal/mole, 200 to 300 sec are required for fifty trajectories.

While the minimum rate constant is in close agreement with some experimental results at 300°K it is above all quoted experimental values. Four independent groups[1-4] give the rate constant at 300°K as $(5.0 \pm 2.0) \times 10^{-11}$, $(5.0 \pm 2.0) \times 10^{-11}$, $(4.3 \pm 1.3) \times 10^{-11}$ and $(3.3 \pm 0.5) \times 10^{-11}$ $cm^3$/molecule sec.; our minimum rate constant is $(5.4 \pm 0.7) \times 10^{-11}$ $cm^3$/molecule sec. As pointed out earlier this calculated rate is definitely low because of the complexes, probably by a factor of two or slightly more. The temperature dependence of the calculated rate constant closely follows the shape of the Kurzius and Boudart[7] curve over all temperatures.

All calculations have been done on a single surface correlating with the ground state of the reactants ($O(^3P) + OH(^2\pi)$), the products ($H(^2S) + O_2\ (^3\Sigma_g^-)$), and the $HO_2$ complex ($^2A''$). The complex has an excited state ($^2A'$) approximately 17 kcal/mole above the ground state ($^2A''$) and this excited state correlates, as does the ground state, with the separated $O(^3P) + OH(^2\pi)$ reactant state. In the $H+O_2$ channel the excited state correlates with the excited $O_2(^1\Delta) + H(^2S)$ state 22.6 kcal/mole above the ground state $O_2(^3\Sigma_g^-) + H(^2S)$. No attempt has been made in these calculations to account for possible transitions to the excited state although the high rate of reaction (above all experimental values) in channel 2 may result from neglect of these transitions.

As more data become available on the $HO_2$ surface through experiment or ab initio calculations improved LEPS semiempirical surfaces can be constructed. In the meantime results such as these reported here help to define the effects of different surface shapes on dynamic calculations.

## REFERENCES


1. M.A.A. Clyne and B.A. Thrush, Proc. Roy. Soc. (London) A275, 544 (1963).

2. F. Kaufman, Ann. Geophys. 20, 106 (1964).

3. J.E. Breen and G.P. Glass, J. Chem. Phys., 52, 1082 (1970).

4. A.A. Westenberg, N. de Haas, and J.M. Roscoe, J. Phys. Chem., 74, 3431 (1970).

5. W.E. Wilson Jr., J. Phys. Chem. Ref. Data 1, 535 (1972).

6. CLASTR is program No. 229 in the Quantum Chemistry Program Exchange Catalog (QCPE, Indiana University Chemistry Department).

7. S.C. Kurzius and M. Boudart, Combust. & Flame, 12, 477 (1968).

8. D.L. Baulich, D.D. Drysdale, and D.G. Horne, Fourteenth Symposium on Combustion (Combustion Institute, Pittsburg, 1973), p. 107.

9. A. Gauss, Jr., J. Chem. Phys. 68, 1689 (1978).

10. J.T. Muckerman, J. Chem. Phys. 56, 2997 (1972).

11. J.F. Ogilvie, Can. J. Spect,, 19, 171 (1973).

12. J.L. Gole and E.F. Hayes, J. Chem. Phys. 57, 360 (1972).

13. A. Gauss, Jr., "The $H+O_2 \rightarrow OH+O$ Reaction, A Comparison of Potential Surfaces", ARBRL-TR- , February 1979 (to be published).

14. J.E. Spencer and G.P. Glass, Internat. J. of Chem. Kinetics, IX, 111 (1977).

15. J.E. Spencer, H. Endo, and G.P. Glass, Sixteenth Symposium on Combustion (Combustion Institute, Pittsburg, 1977) p. 829.

DISTRIBUTION LIST

| No. of Copies | Organization |
|---|---|
| 12 | Commander<br>Defense Documentation Center<br>ATTN: DDC-DDA<br>Cameron Station<br>Alexandria, VA 22314 |
| 1 | Commander<br>US Army Materiel Development and Readiness Command<br>ATTN: DRCDMD-ST<br>5001 Eisenhower Avenue<br>Alexandria, VA 22333 |
| 1 | Commander<br>US Army Aviation Research and Development Command<br>ATTN: DRSAV-E<br>P. O. Box 209<br>St. Louis, MO 63166 |
| 1 | Director<br>US Army Air Mobility Research and Development Laboratory<br>Ames Research Center<br>Moffett Field, CA 94035 |
| 1 | Commander<br>US Army Electronics Research and Development Command<br>Technical Support Activity<br>ATTN: DELSD-L<br>Fort Monmouth, NJ 07703 |
| 1 | Commander<br>US Army Communications Rsch and Development Command<br>ATTN: DRDCO-PPA-SA<br>Fort Monmouth, NJ 07703 |
| 2 | Commander<br>US Army Missile Research and Development Command<br>ATTN: DRDMI-R<br>DRDMI-YDL<br>Redstone Arsenal, AL 35809 |
| 1 | Commander<br>US Army Tank Automotive Rsch and Development Command<br>ATTN: DRDTA-UL<br>Warren, MI 48090 |
| 2 | Commander<br>US Army Armament Research and Development Command<br>ATTN: DRDAR-TSS<br>Dover, NJ 07801 |
| 1 | Commander<br>US Army Armament Materiel Readiness Command<br>ATTN: DRSAR-LEP-L, Tech Lib<br>Rock Island, IL 61299 |
| 1 | Director<br>US Army TRADOC Systems Analysis Activity<br>ATTN: ATAA-SL, Tech Lib<br>White Sands Missile Range<br>NM 88002 |
| 1 | Physical Sciences, Inc.<br>ATTN: Dr. Alan Gelb<br>30 Commerce Way<br>Woburn, MA 01801 |
| 1 | Brookhaven National Laboratory<br>ATTN: Dr. James T. Muckerman<br>Upton, NY 11973 |
| 1 | Texas Tech University<br>Department of Chemistry<br>ATTN: Dr. Thomas O'Brien<br>Lubbock, TX 79409 |
| | Aberdeen Proving Ground<br>Dir, USAMSAA<br>ATTN: Dr. J. Sperrazza<br>DRXSY-MP, H. Cohen<br>Cdr, USATECOM, ATTN: DRSTE-SG-H<br>Dir, Wpns Sys Concepts Team, Bldg. E3516, EA<br>ATTN: DRDAR-ACW |